Science of The Total Environment, Volume 799, 10 December 2021, Article number 149261
DOI:10.1016/j.scitotenv.2021.149261

The mechanisms of struvite biomineralization in municipal wastewater

Authors: Yirong Leng[1], Ana Soares[1]

[1]Cranfield Water Science Institute, Cranfield University, Bedfordshire, MK43 0AL, UK

Abstract

The mechanisms of struvite production by biomineralization were investigated for five microorganisms (*Bacillus pumilus, Brevibacterium antiquum, Myxococcus xanthus, Halobacterium salinarum* and *Idiomarina loihiensis*) in municipal wastewater. The microbial exponential phase of growth occurred within the first 48h of incubation, with growth rates varying from 0.02–0.08 1/h. These five microorganisms removed 23–27 mg/L (66–79%) of ortho-phosphate from wastewater, which was recovered as biological struvite (i.e., bio-struvite) identified by morphological, X-ray diffraction and elemental analysis. Bio-struvite crystals occurred in a low extracellular supersaturation index (0.6–0.8 units). Bio-struvite formation in *B. pumilus M. xanthus*, *H. salinarum* cultures was linked to biologically induced mineralization. Whereas *B. antiquum* and *I. loihiensis* produced bio-struvite through biologically controlled mineralization mechanism because the crystals presented homogeneity in morphology and size, and intracellular vesicle-like cell structures were observed enclosing electron-dense granules/materials. Nutrient recovery through biomineralization has potential application in wastewater streams promoting circularity within the wastewater industry.

[1] Corresponding author at Cranfield Water Science Institute, Cranfield University, Vincent Building, Cranfield, Bedfordshire, MK43 0AL, UK. Tel.: +44 (0) 1234 758121. E-mail address: a.soares@cranfield.ac.uk.

Keywords: Biomineralization; Struvite; Phosphorus recovery; Intracellular cluster；Municipal wastewater

1. Introduction

Struvite ($MgNH_4PO_4.6H_2O$) recovery from wastewater streams has gained attention in recent decades. Struvite deposits as scaling within pipelines and dewatering equipment in wastewater treatment plant (WWTP), particularly in sludge liquor lines of biological nutrient removal processes (Stratful et al., 2001). In these liquors, when concentrations of orthophosphate-phosphorus (PO_4-P), ammonia-nitrogen (NH_4-N) and magnesium (Mg^{2+}) are high enough with solution pH of specific values (e.g. >8.5) in high turbulent areas, the formation of struvite scaling takes place, blocking pipes and equipment spontaneously (Cieślik and Konieczka, 2017; Le Corre et al., 2005). However, struvite is rich in phosphorus (P, 12.6%) and nitrogen (N, 5.7%), and has excellent slow-release property whereby it is capable to reduce P losses from field settings to the surrounding environment (Yetilmezsoy et al., 2017). Furthermore, it may take advantages in terms of energy efficiency and environmental concerns when compared with some nitrogen fixation methods (e.g. thermal plasma nitrogen fixation) (Cherkasov et al., 2015). Therefore it has potential to be used as an alternative to current commercial P and N fertilizer, which can ease dependence on the availability of phosphate rock reserves and the energy consumption in nitrogen fertilizer production (Cherkasov et al., 2015; Massey et al., 2009). Meanwhile, P and N removal from waste streams efficiently minimises the impacts of water pollution (e.g., eutrophication) on environment and ecosystems (Le Corre et al., 2009). Wastewater systems with built-in struvite reactors exist to counteract or mitigate against the problem of the pipe blockages, i.e. stop the waste streams from reaching the component concentrations whereby struvite forms. It was reported that chemical (or abiotic) struvite precipitation removed >90% of PO_4-P (Le Corre et al., 2009), but a minimum PO_4-P >100 mg/L is recommended in wastewater streams for readily struvite crystallization (Rittmann et al., 2011). Furthermore, although the commercial struvite

recovery sector in WWTP has already been large-scale applied, the added chemicals (e.g. sodium hydroxide) for pH control limited potential benefits of struvite production as fertilizer by creating environmental impact (Sena et al., 2021).

As recently more studies focusing on microorganisms' capability of degrading/converting problematic substances to value-added harmless products (Gupta et al., 2019; Kumar et al., 2019), a novel approach of P recovery from wastewater was found to produce struvite through biomineralization (i.e. bio-struvite) (Soares et al., 2014). Compared with abiotic struvite precipitation (e.g., mechanically stirred reactors, fluidized bed reactors) that highly rely on chemical dose and sources of waste streams to achieve high efficiency of P removal (60–94%) (Le Corre et al., 2009), bio-struvite is typically with advantages of high PO_4-P removal (93–95%), recovering P at low concentration (30.5 mg PO_4-P/L) to achieve high P quality effluents (1.5–2.1 mg PO_4-P/L), and no chemical additives to adjust pH (Soares et al., 2014). However, the mechanisms involved in bio-struvite formation in wastewater are still poorly understood.

Cell activity plays a key role in bio-struvite mineralization. Based on the degree of cellular control, biomineralization is traditionally categorised into biologically induced mineralization (BIM) and biologically controlled mineralization (BCM) (Weiner and Dove, 2003). One important feature that distinguishes them is that BCM process occurs in compartmentalized compartments, where specialized regulations of mineral crystallization contribute to the formation of reproducible and species-specific biomineral products (Mann, 2001).

The mechanisms involved in bio-struvite mineralization vary with microbial strains. Specific enzymes (e.g. urease) capable of breaking down nitrogenous organic matters were described to be frequently associated with biomineralization process, by producing ammonia as a metabolic by-product to elevate pH and NH_4-N concentration (Sena et al., 2021). Nevertheless, most bio-struvite crystals was reported to deposit in open environment via BIM process that occurs as a result of interactions between metabolic activity, metabolic by-products and the environment and

has limited control over the type and habit of biominerals (Weiner and Dove, 2003). In particular, cell outer layer was suggested to provide a nucleation and precipitation site for biominerals through negatively charged residues (e.g. polysaccharide) to interact with and accumulate cations (e.g. Mg^{2+}), which is referred to as epicellular mineralization (Mann, 2001). The *Enterobacter sp.* were reported to synthesize bio-struvite through BCM process due to the homogeneity of morphology, composition and mineralogy in crystals (Sinha et al., 2014). Bio-struvite observed in the cytoplasm of *Brevibacterium antiquum* cell (Smirnov et al., 2005), and in the intracellular lipid-rich vesicles of *Paramecium tetraurelia* cell (Grover et al., 1997) were also reported to be associated with BCM process. Because these intracellular vesicles constitute a spatially enclosed environment that maintains a particular ionic composition and allows for increased concentrations of certain ions, thereby fine-tuning the biomineralization process (Mann, 2001). This study aims at understanding the mechanisms of bio-struvite mineralization for selected microbial strains in municipal wastewater, by investigating relationships between microbial growth, cell activity, specific cell structures, solution properties, and characteristics of biomineral products. Wastewater is very complex matrix containing a wide range of organic compounds and ions that can impact biochemical pathways, as well as competing with parallel chemical and physical reactions (Tchobanoglous et al, 2003), consequently with potential to influence the mechanisms of bio-struvite production, when compared with ideal conditions in synthetic media. To the best of our knowledge, this study is the first to explore the mechanisms involved in bio-struvite mineralization from municipal wastewater and provide a comparison between different bacteria under the same conditions.

2. Material and methods

2.1 Wastewater

Municipal wastewater was collected from outlet of primary lamella clarifiers of a municipal WWTP with a 2840-population equivalent (Cranfield, UK). The wastewater was filtered by 10

μm nylon-mesh filter (Plastok, UK), followed by microfiber (equivalent to 0.7 μm), and finally filtered sterilised (0.22 μm PVDF membrane, EMD Millipore, UK). Because the concentrations of PO_4-P, NH_4-N and Mg^{2+} (constituent ions of struvite) in the wastewater used were examined too low to investigate the mechanisms of biomineralization and create supersaturated condition for readily struvite crystallization, these nutrients were added to wastewater based on properties of wastewater previously reported suitable for bio-struvite formation and eligible wastewater sources at WWTP (Table 1) (Fang et al., 2016; Sadowski et al., 2014; Simoes et al., 2017; Soares et al., 2014). Hence, sterile filtered (0.22 μm Minisart® Syringe Filter, Sartorius Stedim Biotech, Germany) concentrated solutions of magnesium sulphate heptahydrate ($MgSO_4 \cdot 7H_2O$), di-potassium hydrogen phosphate (K_2HPO_4), ammonium chloride (NH_4Cl) was supplemented together with bovine serum albumin (BSA) (0.5 g/L) as an organic carbon source for microbial growth. The modified municipal wastewater was used as wastewater source for microbial growth and struvite production in this study. The amendments to the wastewater were kept minimal so any interreference of organic compounds and ions from the wastewater that could impact biochemical pathways or bio-struvite composition would still be present, at the same time ensuring that the quantification and qualification of the bio-struvite could take place and the mechanisms assessed.

2.2 Microorganisms and microbial cultivation

Five microbial strains selected because of their known capability in this study were purchased from commercial culture collections: *Halobacterium salinarum* (DSM 671, German Resource Centre for Biological Material, Germany), *Bacillus pumilus* (GB43, LGC Standards, Middlesex, UK), *Brevibacterium antiquum* (DSM 21545, German Resource Centre for Biological Material, Germany), *Myxococcus xanthus* (CECT 422, Spanish Type Culture Collection, University of Valencia, Paterna, Spain) and *Idiomarina loihiensis* (MAH1/CECT 5996, Spanish Type Culture Collection, University of Valencia, Paterna, Spain). These microorganisms were wild-type strains

isolated from soil or sea water. All these microbial strains were selected because of their known capability to form bio-struvite in solution (González-Muñoz et al., 2008; Soares et al., 2014).

Starter cultures were grown in 250 mL E-flasks containing 100 mL of 4 g/L yeast extract solution (additional 1% w/v NaCl and 1 g/L Mg^{2+} were added to grow *I. loihiensis*), incubated on an orbital shaker (Stuart model SSL1, Fisher Scientific, UK) at agitation rate of 150 RPM and at room temperature (21–22°C) for 96 h. For inoculation in wastewater, the starter cultures were centrifuged (Sanyo MSE Falcon 6/300 centrifuge, 2400 RCF, 4°C, 10 min) and washed with sterile 0.9% w/v NaCl solution. The pure microorganism pellets were re-suspended in wastewater and inoculated in 100 mL glass bottles (Pyrex, Fisher Scientific, UK) containing 36 mL wastewater. Additional 0.8% NaCl was added to *I. loihiensis* culture to ensure its growth (González-Muñoz et al., 2008). The bottles were capped with foam stoppers and incubated on an orbital shaker (Stuart model SSL1, Fisher Scientific, UK) at 150 RPM, room temperature for 192 h. Samples were taken at regular intervals (12–48 h), through sacrificial bottles to minimize sampling errors caused by heterogeneity of crystal produced, especially when completing the particle size distribution analysis. All tests were completed in duplicate and controls were maintained under identical conditions but without inoculation.

2.3 Biological and abiotic struvite preparation, isolation, purification and identification

To prepare enough bio-struvite for crystal identification, 4 L wastewater (eight 1-L glass bottles, each containing 0.5 L wastewater) was used to grow each microbial strain under the identical conditions to those described in section 2.2 for 192 h. At the end of incubation, precipitate was separated from the liquid by filtration (10 μm nylon-mesh filter, Plastok, UK) and washed with deionized (DI) water twice, placed in a drying cabinet with fan at 37-39°C for 4h and finally weighed into aluminium trays.

Abiotic struvite was also prepared in wastewater, with key ions under supersaturation to ensure spontaneous crystallization. Half a litre of raw wastewater containing 50 mM $MgSO_4 \cdot 7H_2O$ (pre-adjusted to pH 9 with 1 M sodium hydroxide) was mixed with 0.25 L wastewater containing 0.2 M ammonium dihydrogen phosphate ($NH_4H_2PO_4$) and 3 mM K_2HPO_4 (pre-adjusted to pH 9 with 1 M sodium hydroxide) in a 1-L glass bottle (Le Corre et al., 2005). The mixture was agitated at 150 RPM at room temperature for 24 h, and abiotic crystals were obtained by the same method that was applied for bio-struvite purification.

Morphological and chemical characterization of the recovered purified precipitate were identified by using a scanning electron microscope equipped with energy dispersive X-ray spectroscopy (SEM-EDX, XL 30 SFEG, Phillips, The Netherlands) and an X-ray powder diffractometer (XRD, D5000, Siemens/Bruker, Germany). The precipitates' chemical composition, including PO_4-P, NH_4-N, Mg^{2+}, calcium (Ca^{2+}) and K^+ was also investigated in 0.22 μm filtrated crystal dissolution (1.25 g/L, prepared in extra pure water pre-adjusted to pH 2 by 1 M hydrogen chloride).

2.4 Analytical methods

Intact cell counts over incubation period were estimated with flow cytometry (BD Accuri C6, BD Biosciences, US) analysis using the SYBR Green I (SG) - propidium iodide (PI) co-staining method (Nocker et al., 2017). The solution pH value was measured using a digital pH-meter (Jenway 3540, Bibby Scientific, UK). After sterile filtration (0.22 μm Minisart® Syringe Filter, Sartorius Stedim Biotech, Germany), concentrations of PO_4-P and NH_4-N were analysed using Smartchem200 (AMS/Alliance Instruments, France) according to manufacturer's instructions, the Mg^{2+}, Ca^{2+} and K^+ were analysed by an atomic absorption spectroscope (AAS, Analyst 800, PerkinElmer, UK) equipped with flaming and electrothermal spectrometers, and soluble chemical oxygen demand (SCOD) was analysed by Spectroquant® test kit (Merck, Germany). The crystal size over time was estimated by volume-based cumulative particle size distribution (D_v) analysis using a Mastersizer 3000 with Hydro EV (Malvern Instruments Ltd, UK). An optical microscope

(Division of GT vision Ltd, UK) was applied for microbial distribution and crystal morphology in fresh culture. For examination of intracellular crystals, the microbial cultures were harvested after 60h incubation, and diluted with DI water to achieve approximately 200–300 cells/μL. A drop of the diluted culture was transferred to a 400-mesh Formvar and carbon-coated copper grid, air-dried and examined by high-resolution transmission electron microscopy (TEM, CM 20, Philips, Japan). A computer application, Visual MINTEQ ver. 3.1 (Gustafsson, 2000), was used to quantify the solution supersaturation index of struvite ($SI_{struvite}$). This application is based on thermodynamic equilibrium comprising Mg^{2+}, Ca^{2+}, PO_4-P, NH_4-N, hydrogen (H^+) and hydroxide (OH^-) with a struvite solubility product constant (K_{sp}) of $10^{-13.26}$ (Ohlinger et al., 1998). Correlations between intact cell count, pH, NH_4-N and PO_4-P were examined using Analysis ToolPak in Excel 2013 (Microsoft, Redmond, Washington, USA), where correlation coefficient (r) more than 0.8 or less than (-0.8) indicate a very strong relationship between variables.

3. Results and discussion

3.1 Microbial growth in municipal wastewater

The selected five microbial strains were observed to grow in wastewater. A lag phase of microbial growth was observed during the first 12 h incubation (except *B. antiquum* and *I. loihiensis* of no lag phase), followed by exponential phase until 48 h (Fig. 1), with estimated growth rates (μ) for the different microorganisms varied from 0.02 (*I. loihiensis*) to 0.03 (*B. pumilus* and *M. xanthus*), to 0.04 (*H. salinarum*) and to 0.08 1/h (*B. antiquum*). The intact cell counts of tested microorganisms were then maintained at a constant level till the end of 192 h incubation (stationary phase) (Fig. 1). The only exception was observed for *M. xanthus*, where a 60% decrease of intact cell counts occurred after 148 h of incubation (Fig. 1), as a signal of cellular autolysis within stationary phase as previously demonstrated (Ben Omar et al., 1995). By the end of incubation period, SCOD was reduced by 150–320 mg/L (Table 2), and more than 90% of the

SCOD reduction occurred during the exponential phase of microbial growth. Neither intact cell counts nor SCOD reduction was observed in the non-inoculated controls.

In this study, *B. antiquum* presented the highest growth rate (μ=0.08 1/h) and shortest lag phase compared with the other four microorganisms (Fig. 1). This growth rate was the same order of magnitude than previously reported value (μ=0.06 1/h) in wastewater where *B. antiquum* took acetate as major carbon source (equivalent to 1000 mg/L chemical oxygen demand) (Simoes et al., 2017). In contrast to *B. antiquum*, *I. loihiensis* presented low growth rate (μ=0.02 1/h) in wastewater (Fig. 1). Growth of *I. loihiensis* requires relatively high NaCl concentration (0.7–20% w/v), and could be favoured in municipal wastewater with salinities of 2 % w/v NaCl (González-Muñoz et al., 2008). The BSA (as additional carbon source) was suggested to contribute to microbial growth in wastewater. Most of the investigated microorganisms can use BSA as a carbon source (Leng et al., 2020). A previous study reported lower growth rates (μ ≤0.004 1/h) for four of the selected microorganisms in wastewater streams with no extra carbon source, although a different method (turbidity measurement) was used (Soares et al., 2014). However, microbial growth rates in wastewater were 60–90% lower than those in synthetic solution (μ=0.16–0.28 1/h) where yeast extract was used as a carbon source (Leng and Soares, 2021). Compared with BSA, yeast extract not only provides protein but also vitamins (e.g. B1, B2, B6, niacin, folic acid) and minerals (e.g. iron, zinc) as essential macro/micronutrients for microbial growth (EURASYP, 2014). Shortage of such nutrients might have limited the microbial growth in wastewater, but further investigations are required to determine which factors limited the microbial growth.

3.2 Crystal identification and morphology

All the selected microorganisms produced crystals in wastewater (Fig. SA. 1-5). No precipitate was observed in the non-inoculated controls. The dominant biologically produced crystals possessed the same elongated trapezoidal platy shape as the struvite previously described

(Kemacheevakul et al., 2015). An observation of large long-bar shaped crystals in *I. loihiensis* culture was also mentioned previously in marine medium (González-Muñoz et al., 2008). Furthermore, XRD results showed that the crystals had similar peak profiles to standard struvite (pattern COD 9007674) (Fig. SB). Thus, the supersaturated minerals in wastewater inoculated with the microorganisms were clearly identified as struvite. A detailed analysis of the crystal morphology face expressions showed that [022] ([011]), [012] and [111] were the dominant faces (Fig. SA. 1). Struvite was observed to have an asymmetric structure, owing to its internal atomic arrangement (Prywer and Torzewska, 2009). In this study, crystal growth was observed to elongate along the a-axis and asymmetric along the c-axis. Although truncated apices appeared at bio-struvite crystals for all microbial cultures in this study (Fig. 2 a–b), as a signal that the crystals had lost their rectangular symmetry. Microorganisms were capable to exert influence on struvite morphology by molecular electrostatic interactions between molecular structures of crystal surface (e.g. [011] face terminated by NH_4^+, [00$\overline{1}$] face with high density of Mg^{2+}) and negatively charged microbial cell out-layer or extracellular polymers (e.g. polysaccharide of *Proteus mirabilis*) (Prywer and Torzewska, 2009). The secretion of phosphate groups by phosphatase activity has also been reported to contribute to the electronegative charged density of cell outer-layer (Macaskie et al., 2000). In this study, the enhanced crystal faces suggested a preference of microbial cells bounding to specific faces during bio-struvite crystal growth in wastewater. Such selective interactions between microbial cells and the molecular structure of crystal surface slowed down growth of specific crystal faces (e.g. [011]), which lead to elongated trapezoidal platy shaped crystals. Abiotic struvite, on the other hand, was found to be mainly dendritic crystals (Fig. 2 f). Such morphology was previously reported to frequently occur at pH ≥9 (Prywer and Torzewska, 2009), and it indicated a diffusion-controlled crystal growth where the growth of certain edges and corners of crystals was enhanced in the direction of high supersaturation along the same lattice, as previously described (Shaddel et al., 2019).

Parallel grouping and various types of twinning were observed during the stationary phase of microbial growth, including parallel grouping (Fig. 2 a), penetrate twining (Fig. 2 b), cyclic twining (Fig. 2 d) and contact twining (Fig. 2 e), with contact twining along $[00\bar{1}]$ faces being the most common twining types. Contact twining and penetrate twining of bio-struvite were reported to occur at pH 9 and above (Prywer and Torzewska, 2010), although occurrences of twinning in this study were observed at lower pH (8.2–8.4). Both parallel grouping and twinning encouraged the formation of large crystals and morphology evolution, along with an occurrence of Ostwald ripening that was proposed for crystal surface smoothing.

The bio-struvite recovered from wastewater and its abiotic counterpart were further examined by a standard chemical way to compare their properties. The component element analysis (based on weight percent, wt %) presented similar stoichiometric ratios $[Mg^{2+}]$:$[PO_4$-P$]$:$[NH_4$-N] about 1:1:1 in crystal dissolution and [Mg]:[P]:[O] about 1:1:(4–6) within crystal surface structures (nitrogen under limit of detection by SEM-EDX) (Table SA). Therefore, the crystals biologically produced in wastewater by the investigated microbial strains were similar to the abiotic struvite standard. A detected significant loss of nitrogen and oxygen in composition within the surface crystalline framework (as ammonia and molecule water) in this study was due to the air-drying method applied (section 2.3), as previously reported (Frost et al., 2004).

The purity of bio-struvite produced by the five selected microbial strains in wastewater was affected by Ca^{2+} and K^+ (measured at Ca^{2+} of 36.6 mg/L and K^+ of 93.1 mg/L). Low content of Ca^{2+} (0.8 mg/g) and K^+ (0.2 mg/g) (Table SA) were also detected in abiotic struvite precipitated in wastewater (measured at Ca^{2+} of 36.6 mg/L and K^+ of 100 mg/L). Compared with abiotic struvite, the bio-struvite presented higher content of K^+ (0.6–0.8 mg/g) and lower content of Ca^{2+} (0.1–0.2 mg/g) (Table SA). The detected relatively high K^+ content in bio-struvite was related to the K^+ uptake and accumulation within microbial cells (Britto and Kronzucker, 2008), whereby more K^+ could be released to crystalline framework when the cells bonded to crystal surface via

specific molecular interactions (Sadowski et al., 2014). While an observed relatively high content of Ca^{2+} (0.8 mg/g) in abiotic struvite was due to specific composition of the wastewater ($[Mg^{2+}]$:$[Ca^{2+}]$ about 2.5:1), which may result in precipitation of a considerable amount of amorphous calcium phosphates (Ca-P) on the abiotic struvite, introducing impurity into crystals (Le Corre et al., 2005).

3.3 Bio-struvite production in wastewater and solution supersaturation

By the end of 192 h incubation, the selected microorganisms produced 120–150 mg bio-struvite crystals (≥10 μm) per litre of wastewater treated, corresponding to nutrients' recovery of 12–19 mg/L PO_4-P and 9–15 mg/L Mg^{2+} from wastewater (Table 2). The bio-struvite yields in this study were comparable to previously reported bio-struvite production (196±25, 198±42, 135±12 mg/L for *B. pumilu*s, *H. salinarum*, and *B. antiquum*, respectively) in sludge dewatering liquors containing similar initial Mg^{2+} and PO_4-P and pH but with a 2.1–2.7 fold initial NH_4-N (Simoes, 2017). An equal decrease in molar concentration of PO_4-P and Mg^{2+} (Table 2) well corresponded with the stoichiometric molar ratio of $[Mg^{2+}]$:$[PO_4$-P] (1:1) of recovered bio-struvite (Table SA). The most significant drop of PO_4-P (62–73%) and Mg^{2+} (25–28%) occurred within the microbial exponential phase (48 h) (Fig. 3 a–b). The pH increased rapidly from initial units of 7.6–7.7 to units of 8.1–8.3 (36 h) during the exponential phase, and maintained a constant level (pH 8.2–8.4) until the end of incubation period (Fig. 3 c). The variation of NH_4-N concentration with time (Fig. 3 d) represented a same trend as the pH profile. Neither precipitant nor variation of pH, NH_4-N, Mg^{2+} and PO_4-P was observed in non-inoculated wastewater.

During the microbial exponential phase, very strong positive correlations ($r \geq 0.90$) between intact cell count, NH_4-N and pH were obtained; whereas these three variables were significantly negatively correlated with PO_4-P and Mg^{2+} ($r \leq 0.80$) (Table SB), indicating that the variations of pH, NH_4-N, PO_4-P and Mg^{2+} were highly dependent on microbial growth. In this study, an observed microbial growth (Fig. 1) resulted in decomposition of nitrogen compounds to increase

pH (Fig. 3 c) and release NH_4^+ (Fig. 3 d), which integrated with PO_4-P and Mg^{2+} presented in wastewater to form struvite when supersaturation conditions achieved, thus the drop of concentrations of PO_4-P (Fig. 3 a) and Mg^{2+} (Fig. 3 b) as a result of struvite formation, as previously described (Sinha et al., 2014). The PO_4-P removal and recovery in this study varied from 23 (*I. loihiensis*) to 27 (*B. antiquum*) mg PO_4-P/L wastewater, and 12 (*M. xanthus*) to 19 (*H. salinarum*) mg PO_4-P/L wastewater, respectively. The *B. antiquum* was reported to be capable of using organic and condensed P, besides PO_4-P, with organic and condensed P contributing to 48% of the P recovered by bio-struvite (Simoes, 2017). Thus the capability of microorganisms to remove and recover P as bio-struvite from wastewater streams might be underestimated in this study, provided that they could make use of, beside the inorganic P, the organic P that typically makes up 1–5 mg/L of the total P of 5–20 mg/L in municipal wastewater (Ivanov et al., 2005).

As a result of variations of pH and concentrations of PO_4-P, NH_4-N and Mg^{2+}, the solution (or extracellular) $SI_{struvite}$ initiated from values of 0.4 (*I. loihiensis*) and 0.5 (for the other four microbial strains), and peaked at values between 0.7 (*I. loihiensis*, 36h) and 0.8 (*B. antiquum*, 36h) during the exponential phase of growth (24–48 h); the solution $SI_{struvite}$ then steadily decreased to values between 0.4 (*H. salinarum*) and 0.5 (*M. xanthus*) by the end of 192 h (Fig. 3 e). Bio-struvite crystals were observed to occur in microbial cultures during 12–24 h incubation, when the solution $SI_{struvite}$ raised to values between 0.6 and 0.8 (Fig. 3 e). The solution $SI_{struvite}$ eligible for bio-struvite formation in wastewater in this study was within a similar range as those previously investigated in synthetic solution ($SI_{struvite}$=0.6–0.8) (Leng and Soares, 2021). Furthermore, the solution $SI_{struvite}$ required for bio-struvite mineralization in this study is of much lower values than those previously reported for abiotic struvite spontaneous precipitation (e.g. $SI_{struvite} \geq 1.2$) (Galbraith and Schneider, 2009) and for pilot-scale optimized P recovery by struvite (e.g. $SI_{struvite}$=2–6) (Bhuiyan et al., 2008), indicating preferential occurrence of bio-struvite nucleation at relatively low $SI_{struvite}$ in streams. A potential formation of calcium hydroxyapatite (HAP) was assumed based on high solution SI of HAP (11–14) and reduction of Ca^{2+} (2–8 mg/L) in

inoculated wastewater (Fig. 3 f), although no HAP crystals was identified. The presence of Ca^{2+} was reported to hinder bio-struvite production due to a priority of mineral precipitation (Rivadeneyra et al., 2006). However, in this study, it is noted that the molar ratio of removed $[Mg^{2+}]$:$[Ca^{2+}]$ from wastewater by *B. antiquum* (18 units) was higher than the other microbial strains (6–10 units), indicating that *B. antiquum* produced mineral containing more Mg^{2+} and less Ca^{2+} content.

3.4 Bio-struvite growth

A rapid crystal growth occurred within the first 72 h of incubation (Fig. 4 a–b). It was followed by constant levels of cumulative crystal size distribution that was maintained until the end of incubation period, achieving final D_{v50} (median particle size by volume distribution) of bio-struvite crystals produced by *H. salinarum, M. xanthus, B. pumilus, B. antiquum* and *I. loihiensis* bio-struvite of 178±4, 163±6, 138±1, 131±7 and 85±4 μm (Fig. 4 a), respectively, and final D_{v90} of 451±27, 420±7, 402±8, 254±2 and 212±5 μm, respectively. The percentage of bio-struvite crystals above 100 μm increased from initial 0 to final 41–46% of total particles in solution (Fig. 4 b). Compared with bio-struvite, the abiotic struvite was relatively small with an average size of around 50 μm (Fig. 2 f).

The crystal growth was further studied via gap range between D_{v50} and D_{v90} (i.e., Dv_{90} - Dv_{50}) obtained from final crystal size distribution, whereby *B. antiquum* (123 μm) and *I. loihiensis* (127 μm) distinguish themselves from *H. salinarum* (273 μm), *B. pumilus* (264 μm) and *M. xanthu*s (257 μm) by relative narrow gap ranges and uniform size. Furthermore, an overview of bio-struvite crystals produced by *B. antiquum* and *I. loihiensis* showed better reproducibility in terms of size and morphology, whereas the other three microbial strains produced bio-struvite with heterogeneity (Fig. SA). Homogeneity of morphology, size and composition are important features of BCM process (Weiner and Dove, 2003), whereby magnetotactic bacteria was distinguished from iron-reducing bacteria in magnetite synthesis (Frankel and Bazylinski, 2003).

The observation of bio-struvite crystals with size and morphological homogeneity in this study suggested a link between manipulation of microbial growth and recovery of nutrients by bio-struvite of controlled quality from wastewater. When comparing the bio-struvite growth in wastewater with previously reported in synthetic solution, it was observed that the crystals produced during microbial stationary phase were of similar D_{v50} and D_{v90} in both streams, but the percentages of large crystal group (≥100 μm) of bio-struvite in wastewater were reduced by from 12% (*B. antiquum*) to 41% (*H. salinarum*), and the reaction time required to reach constant level of crystal size distribution was extended by 24–48h in wastewater (Leng and Soares, 2021).

Crystal size and the size distribution were highly affected by supersaturation levels of liquid streams. High supersaturation (e.g. $SI_{struvite}$ =2.8) preferred nucleation (especially homogeneous nucleation) over crystal growth, and the enhanced nucleation dominated in competition with crystal growth for component elements (Ohlinger et al., 1999; Ronteltap et al., 2010). In this study, the observed large amount of abiotic struvite particles of small size (Fig. SA. 6) resulted from high supersaturation level (SI>4) of wastewater. However, efficient solid-liquid separation preferred crystals of large size to minimise the loss of crystals during washing out and ensure minimum P content in effluent (Shaddel et al., 2019). To optimize the crystal production and benefit crystal growth, seeded crystallization (e.g. struvite fines) was introduced to lower levels of supersaturation for heterogeneous nucleation (e.g. $SI_{struvite}$ =1.55) and to shorten induction time (Mehta and Batstone, 2013). In this study, heterogeneous nucleation of bio-struvite was observed during the first 24h incubation at relative low levels of supersaturation ($SI_{struvite}$ =0.6–0.8), and was followed by crystal growth within even lower range of $SI_{struvite}$ (0.4–0.8) (Fig. 3 e). The relative low supersaturation levels benefitted crystals' settling properties such as larger size, lower content of fine particles and morphology (e.g. bipyramidal) (Shaddel et al., 2019). In addition, microbial cells may have potential to serve as bio-seeds for struvite production. Compared with abiotic seeds, the microbial cells/cell debris (e.g. *Myxococcus* cells) in streams not only act as heterogeneous nuclei by providing surface, but also enable interactions between solution ions and

cell surface or charged substance secreted/functioned by cells, accumulating mineral precipitate on/inside cells (Ben Omar et al., 1995; Frankel and Bazylinski, 2003). Furthermore, provided that the crystal nucleus depends on microbial cells, the number of bio-struvite crystals might be relative to microbial growth.

3.5 Bio-struvite biomineralization mechanisms in wastewater

Two possible mechanisms, biologically induced mineralization and biologically controlled mineralization, were involved in bio-struvite biomineralization in this study: microorganisms alter solution chemistry (e.g., pH, NH_4^+) by metabolic activities, whereby PO_4^{3-} and Mg^{2+} integrated with NH_4^+ to form struvite when supersaturation conditions were achieved in solution or within intracellular compartment membrane (Fig. SC). When comparing the key features of bio-struvite mineralization in wastewater with those in synthetic solutions (Leng and Soares, 2021), no significant changes regarding mechanisms involved in biomineralization process was observed: microbial growth produced NH_4-N and increased pH, the BCM bio-struvite formation (*B. antiquum* and *I. loihiensis*) was distinguished from BIM bio-struvite formation (*H. salinarum*, *B. pumilus* and *M. xanthus*) by homogeneity of crystals (e.g. size, morphology) and signature cell structures (e.g. intracellular vesicles enclosing electron dense clustered materials) (Table 3).

Intracellular spherical structures within the membrane observed within *B. antiquum* and *I. loihiensis* cells in wastewater are suggested to be lipid vesicles, due to similar structure to previously reported lipid vesicles (Spiegel et al., 2013). Some of these cell structures were identified containing electron dense granules/materials (Fig. 5 a–b), and the dense granules inside the vesicle-like structures were morphologically similar to the intracellular bio-struvite crystals in *P. tetraurelia* cells (Grover et al., 1997). Observation of intracellular vesicles during biomineralization suggests highly biological control over the process, for example magnetosome vesicles produced by magnetotactic bacteria enable controlled intracellular iron transportation to form magnetosome crystals that were characterised as BCM minerals (e.g. narrow size ranges,

high chemical purity, morphological homogeneity) (Bazylinski and Frankel, 2003). The formation of *B. antiquum* and *I. loihiensis* bio-struvite in wastewater was here suggested to be BCM process. Neither intracellular membrane structures nor intracellular electron-dense cluster was observed in yeast extract solution used to grow *B. antiquum* and *I. loihiensis*, and in inoculated wastewater of the other three investigated microbial strains in this study.

BIM process takes place in an open environment, and occurs as a result of interactions between metabolic activity and local environment, typically by various metabolic products (e.g. pH, carbon dioxide, nitrogen compounds) extruding across the cell membrane via active pumping or passive diffusion to interact with ions and compounds presented in the environment (Frankel and Bazylinski, 2003). The lack of cellular control in BIM process often leads to adventitiously precipitation of minerals with poorly defined mineral specificity and crystallinity (e.g., inclusion of impurity), and heterogeneity in mineral morphology and size (Frankel and Bazylinski, 2003). *B. pumilis*, *M. xanthus* and *H. salinarum* cultures were linked to BIM as the size distribution and shape of crystals was heterogenous and it was not observed the presence of intracellular membrane structures nor intracellular electron-dense clusters. The fact that mineralisation was observed, in the presence of cells, and not in the uninoculated controls, indicates that the process was biologically induced. Crusted two-cell and tetrad cell clusters in *B. pumilus* culture, observed with potential to form aggregates in wastewater (Fig. 5 c) were morphologically similar to the biominerals formed in *Thiomargarita* embryo infestation (Bailey et al., 2007) and microbial silicification (Yee et al., 2003). In biomineralization process, bacteria cells were reported to be partially to completely encrusted by materials such as iron-rich capsule, granules structure and siliceous spheroidal crystallite spheroids embedded within iron-rich capsular material or spheres (Konhauser and Riding, 2012). Characterized by an anionic thick outer layer (about 25 nm wide peptidoglycan framework), the *B. pumilus* cell had potential to form a thick and robust mineral crust around itself (Schultze-Lam et al., 1996; Westall, 1999). The crusted cell structures in *B. pumilus* culture were therefore proposed as a result of extensive epicellular mineralization in

wastewater. However, as a most characterized BIM process, the process and mineral products of epicellular mineralization were highly dependent on the environment (Mann, 2001).

In this study, the microorganisms made use of wastewater enriched with BSA as a carbon source to grow, indicating that the microbes can adapt to wastewater. This study revealed a capability of the investigated microorganisms to produce bio-struvite of high quality and large size in wastewater of low levels of PO_4-P and $SI_{struvite}$, without chemical dosing for pH adjustment. Chemical precipitation is currently the most common way to produce struvite in wastewater streams, but the efficiency is highly reliant on pH and nutrient concentrations (Mehta et al., 2015). The application of bio-struvite in municipal wastewater can remove P and N without additional cost for pH adjustment and PO_4-P elevation, along with reduction of chemical oxygen demand as an additional benefit. Furthermore, the occurrence of BCM bio-struvite in wastewater links microbial growth with bio-struvite quality (e.g., purity, morphology), typically by producing lipid vesicles where chemical regulations can be applied on biomineral products. Besides creating an isolated micro-environment, the BCM processes generally highly rely on positive pumping of specific ions (Mann, 2001). Thus, the two bacteria (*B. antiquum* and *I. loihiensis*) that are proposed to be involved in BCM bio-struvite formation have a potential to remove/recover nutrients from raw municipal wastewater with low PO_4-P concentration (e.g. 4–15 mg/L) (Henze and Comeau, 2008) and produce bio-struvite of more controlled quality.

4. Conclusions and Prospects

- Growth of the selected microorganisms (μ=0.02–0.08 1/h) in municipal wastewater benefited bio-struvite production and reduced supersaturation barrier for heterogenous nucleation ($SI_{struvite}$ =0.6–0.8).

- Wastewater affected bio-struvite crystal properties in terms of morphology, purity and size distribution. Elongated trapezoidal platy shaped crystals dominated the bio-struvite mineral products.

- Wastewater had limited influence on mechanisms involved in the biomineralization. *H. salinarum*, *B. pumilus* and *M. xanthus* were identified as producing bio-struvite via BIM process. The formation of *B. antiquum* and *I. loihiensis* bio-struvite in wastewater, based on the observation of intracellular vesicle-like structures and homogeneity in terms of crystal morphology and size, was identified as BCM process.

- Observation of high biological control over the bio-struvite mineralization of *B. antiquum* and *I. loihiensis* in wastewater open opportunities for resources recovery from wastewater by high-qualified bio-struvite crystals as value-added products.

- The capability of selected microorganisms to produce struvite of high quality in wastewater in combination with recent study for their biochemical characterization provides links between bio-struvite production at WWTP and development of design of reactors/processes and operational conditions for optimising growth of specific microbial strains in mixed cultures.

References

Bailey, J. V., Joye, S.B., Kalanetra, K.M., Flood, B.E., Corsetti, F.A., 2007. Evidence of giant sulphur bacteria in Neoproterozoic phosphorites. Nature 445, 198–201. https://doi.org/10.1038/nature05457

Bazylinski, D. a., Frankel, R.B., 2003. Biologically controlled mineralization in prokaryotes, in: Reviews in Mineralogy and Geochemistry. pp. 217–247. https://doi.org/10.2113/0540217

Ben Omar, N., Martínez-Cañamero, M., González-Muñoz, M.T., Maria Arias, J., Huertas, F., 1995. Myxococcus xanthus' killed cells as inducers of struvite crystallization. Its possible

role in the biomineralization processes. Chemosphere 30, 2387–2396. https://doi.org/10.1016/0045-6535(95)00110-T

Bhuiyan, M.I.., Mavinic, D.., Koch, F.., 2008. Phosphorus recovery from wastewater through struvite formation in fluidized bed reactors: A sustainable approach. Water Sci. Technol. 57, 175–181. https://doi.org/10.2166/wst.2008.002

Britto, D.T., Kronzucker, H.J., 2008. Cellular mechanisms of potassium transport in plants. Physiol. Plant. 133, 637–650. https://doi.org/10.1111/j.1399-3054.2008.01067.x

Cherkasov, N., Ibhadon, A.O., Fitzpatrick, P., 2015. A review of the existing and alternative methods for greener nitrogen fixation. Chem. Eng. Process. Process Intensif. 90, 24–33. https://doi.org/10.1016/j.cep.2015.02.004

Cieślik, B., Konieczka, P., 2017. A review of phosphorus recovery methods at various steps of wastewater treatment and sewage sludge management. The concept of "no solid waste generation" and analytical methods. J. Clean. Prod. 142, 1728–1740. https://doi.org/10.1016/j.jclepro.2016.11.116

EURASYP, 2014. Natural yeast – the nutritious basis for yeast extract [WWW Document]. URL http://www.yeastextract.info/news-and-downloads/news/135/natural-yeast-the-nutritious-basis-for-yeast-extract (accessed 2.1.21).

Fang, C., Zhang, T., Jiang, R., Ohtake, H., 2016. Phosphate enhance recovery from wastewater by mechanism analysis and optimization of struvite settleability in fluidized bed reactor. Sci. Rep. 6, 1–10. https://doi.org/10.1038/srep32215

Frankel, R.B., Bazylinski, D.A., 2003. Biologically induced mineralization by bacteria, in: Reviews in Mineralogy and Geochemistry. pp. 95–114. https://doi.org/10.2113/0540095

Frost, R.L., Weier, M.L., Erickson, K.L., 2004. Thermal decomposition of struvite: Implications for the decomposition of kidney stones. J. Therm. Anal. Calorim. 76, 1025–1033.

https://doi.org/10.1023/B:JTAN.0000032287.08535.b3

Galbraith, S.C., Schneider, P.., 2009. A review of struvite nucleation studies, in: International Conference on Nutrient Recovery from Wastewater Streams. IWA publishing, London, UK, pp. 69–78.

González-Muñoz, M.T., De Linares, C., Martínez-Ruiz, F., Morcillo, F., Martín-Ramos, D., Arias, J.M., 2008. Ca-Mg kutnahorite and struvite production by Idiomarina strains at modern seawater salinities. Chemosphere 72, 465–472. https://doi.org/10.1016/j.chemosphere.2008.02.010

Grover, J.E., Rope, a F., Kaneshiro, E.S., 1997. The occurrence of biogenic calcian struvite, (Mg,Ca)NH4PO4.6H2O, as intracellular crystals in Paramecium. J. Eukaryot. Microbiol. 44, 366–373.

Henze, M., Comeau, Y., 2008. Wastewater characterization, in: Biological Wastewater Treatment: Principles Modelling and Design. IWA publishing, pp. 33–52.

Ivanov, V., Stabnikov, V., Zhuang, W.Q., Tay, J.H., Tay, S.T.L., 2005. Phosphate removal from the returned liquor of municipal wastewater treatment plant using iron-reducing bacteria. J. Appl. Microbiol. 98, 1152–1161. https://doi.org/10.1111/j.1365-2672.2005.02567.x

Kemacheevakul, P., Chuangchote, S., Otani, S., Matsuda, T., Shimizu, Y., 2015. Effect of magnesium dose on amount of pharmaceuticals in struvite recovered from urine. Water Sci. Technol. 72, 1102–1110. https://doi.org/10.2166/wst.2015.313

Konhauser, K., Riding, R., 2012. Bacterial biomineralization, in: H., A., Donald, K., Canfield, E., Konhauser, K.O. (Eds.), Fundamentals of Geobiology. Blackwell Publishing Ltd, pp. 105–130. https://doi.org/10.1002/9781118280874.ch8

Le Corre, K.S., Valsami-Jones, E., Hobbs, P., Parsons, S. a., 2009. Phosphorus recovery from wastewater by struvite crystallization: a Review. Crit. Rev. Environ. Sci. Technol. 39, 433–

477. https://doi.org/10.1080/10643380701640573

Le Corre, K.S., Valsami-Jones, E., Hobbs, P., Parsons, S. a., 2005. Impact of calcium on struvite crystal size, shape and purity. J. Cryst. Growth 283, 514–522. https://doi.org/10.1016/j.jcrysgro.2005.06.012

Leng, Y., Colston, R., Soares, A., 2020. Understanding the biochemical characteristics of struvite bio-mineralising microorganisms and their future in nutrient recovery. Chemosphere 247, 125799. https://doi.org/10.1016/j.chemosphere.2019.125799

Leng, Y., Soares, A., 2021. Understanding the mechanisms of biological struvite biomineralisation. Chemosphere 281, 130986. https://doi.org/10.1016/j.chemosphere.2021.130986

Macaskie, L.E., Bonthrone, K.M., Yong, P., Goddard, D.T., 2000. Enzymically mediated bioprecipitation of uranium by a Citrobacter sp.: A concerted role for exocellular lipopolysaccharide and associated phosphatase in biomineral formation. Microbiology 146, 1855–1867. https://doi.org/10.1099/00221287-146-8-1855

Mann, S., 2001. Biomineralization : principles and concepts in bioinorganic materials chemistry. Oxford University Press.

Massey, M.S., Davis, J.G., Ippolito, J.A., Sheffield, R.E., 2009. Effectiveness of recovered magnesium phosphates as fertilizers in neutral and slightly alkaline soils. Agron. J. 101, 323–329. https://doi.org/10.2134/agronj2008.0144

Mehta, C.M., Batstone, D.J., 2013. Nucleation and growth kinetics of struvite crystallization. Water Res. 47, 2890–2900. https://doi.org/10.1016/j.watres.2013.03.007

Mehta, C.M., Khunjar, W.O., Nguyen, V., Tait, S., Batstone, D.J., 2015. Technologies to recover nutrients from waste streams: A critical review. Crit. Rev. Environ. Sci. Technol. 45, 385–427. https://doi.org/10.1080/10643389.2013.866621

Nocker, A., Cheswick, R., Dutheil de la Rochere, P.M., Denis, M., Léziart, T., Jarvis, P., 2017. When are bacteria dead? A step towards interpreting flow cytometry profiles after chlorine disinfection and membrane integrity staining. Environ. Technol. 38, 891–900. https://doi.org/10.1080/09593330.2016.1262463

Ohlinger, B.K.N., Member, S., Young, T.M., Member, A., Schroeder, E.D., 1999. Kinetics effects on preferential struvite accumulation in wastewater. J. Environ. Eng. 125.

Ohlinger, K.N., Young, T.M., Schroeder, E.D., 1998. Predicting struvite formation in digestion. Water Res. 32, 3607–3614. https://doi.org/10.1016/S0043-1354(98)00123-7

Prywer, J., Torzewska, A., 2010. Biomineralization of struvite crystals by Proteus mirabilis from artificial urine and their mesoscopic structure. Cryst. Res. Technol. 45, 1283–1289. https://doi.org/10.1002/crat.201000344

Prywer, J., Torzewska, A., 2009. Bacterially induced struvite growth from synthetic urine: experimental and theoretical characterization of crystal morphology. Cryst. Growth Des. 9, 3538–3543. https://doi.org/10.1021/cg900281g

Rittmann, B.E., Mayer, B., Westerhoff, P., Edwards, M., 2011. Capturing the lost phosphorus. Chemosphere 84, 846–853. https://doi.org/10.1016/j.chemosphere.2011.02.001

Rivadeneyra, M.A., Delgado, R., Párraga, J., Ramos-Cormenzana, A., Delgado, G., 2006. Precipitation of minerals by 22 species of moderately halophilic bacteria in artificial marine salts media: Influence of salt concentration. Folia Microbiol. (Praha). 51, 445–453. https://doi.org/10.1007/BF02931589

Ronteltap, M., Maurer, M., Hausherr, R., Gujer, W., 2010. Struvite precipitation from urine - Influencing factors on particle size. Water Res. 44, 2038–2046. https://doi.org/10.1016/j.watres.2009.12.015

Sadowski, R.R., Prywer, J., Torzewska, A., 2014. Morphology of struvite crystals as an evidence

of bacteria mediated growth. Cryst. Res. Technol. 49, 478–489. https://doi.org/10.1002/crat.201400080

Schultze-Lam, S., Fortin, D., Davis, B., Beveridge, T., 1996. Mineralization of bacterial surfaces. Chem. Geol. 132, 171–181. https://doi.org/10.1016/S0009-2541(96)00053-8

Sena, M., Seib, M., Noguera, D.R., Hicks, A., 2021. Environmental impacts of phosphorus recovery through struvite precipitation in wastewater treatment. J. Clean. Prod. 280, 124222. https://doi.org/10.1016/j.jclepro.2020.124222

Shaddel, S., Ucar, S., Andreassen, J.P., Sterhus, S.W., 2019. Engineering of struvite crystals by regulating supersaturation - Correlation with phosphorus recovery, crystal morphology and process efficiency. J. Environ. Chem. Eng. https://doi.org/10.1016/j.jece.2019.102918

Simoes, F., 2017. A new route to recover phosphorus from waste water: biological struvite production School. Cranfield University.

Simoes, F., Vale, P., Stephenson, T., Soares, A., 2017. Understanding the growth of the bio-struvite production Brevibacterium antiquum in sludge liquors. Environ. Technol. 39, 1–10. https://doi.org/10.1080/09593330.2017.1411399

Sinha, A., Singh, A., Kumar, S., Khare, S.K., Ramanan, A., 2014. Microbial mineralization of struvite: a promising process to overcome phosphate sequestering crisis. Water Res. 54, 33–43. https://doi.org/10.1016/j.watres.2014.01.039

Smirnov, A., Suzina, N., Chudinova, N., Kulakovskaya, T., Kulaev, I., 2005. Formation of insoluble magnesium phosphates during growth of the archaea Halorubrum distributum and Halobacterium salinarium and the bacterium Brevibacterium antiquum. FEMS Microbiol. Ecol. 52, 129–137. https://doi.org/10.1016/j.femsec.2004.10.012

Soares, A., Veesam, M., Simoes, F., Wood, E., Parsons, S. a., Stephenson, T., 2014. Bio-Struvite: A new route to recover phosphorus from wastewater. Clean - Soil, Air, Water 42, 994–997.

https://doi.org/10.1002/clen.201300287

Spiegel, C.N., Bretas, J.A.C., Peixoto, A.A., Vigoder, F.M., Bruno, R. V., Soares, M.J., 2013. Fine structure of the male reproductive system and reproductive behavior of Lutzomyia longipalpis sandflies (Diptera: Psychodidae: Phlebotominae). PLoS One 8, e74898. https://doi.org/10.1371/journal.pone.0074898

Stratful, I., Scrimshaw, M.D., Lester, J.N., 2001. Conditions influencing the precipitation of magnesium ammonium phosphate. Water Res. 35, 4191–4199. https://doi.org/10.1016/S0043-1354(01)00143-9

Tchobanoglous, G., Burton, F. L. and Stensel, H. D. 2003. Wastewater engineering: treatment and reuse. 4th, Inter edn. Edited by G. Tchobanoglous, F. Franklin L. Burton, and H. D. Stensel. New York: McGraw-Hill Higher Education (The McGraw-Hill Series in Civil and Environmental Engineering).

Weiner, S., Dove, P.M., 2003. An overview of biomineralization processes and the problem of the vital effect, in: Reviews in Mineralogy and Geochemistry. pp. 1–29. https://doi.org/10.2113/0540001

Westall, F., 1999. The nature of fossil bacteria: A guide to the search for extraterrestrial life. J. Geophys. Res. 104451, 437–16. https://doi.org/10.1029/1998JE900051

Yee, N., Phoenix, V.R., Konhauser, K.O., Benning, L.G., Ferris, F.G., 2003. The effect of cyanobacteria on silica precipitation at neutral pH: Implications for bacterial silicification in geothermal hot springs. Chem. Geol. 199, 83–90. https://doi.org/10.1016/S0009-2541(03)00120-7

Yetilmezsoy, K., Ilhan, F., Kocak, E., Akbin, H.M., 2017. Feasibility of struvite recovery process for fertilizer industry: A study of financial and economic analysis. J. Clean. Prod. 152, 88–102. https://doi.org/10.1016/j.jclepro.2017.03.106

Table 1 Chemical properties of the wastewater and element analysis of crystal dissolution of bio-struvite and abiotic struvite recovered from wastewater. Nutrients were added to the wastewater to investigate the mechanisms biomineralization in optimal conditions and hence avoid interreference of limiting nutrients.

	pH	SCOD (mg/L)	PO_4-P (mg/L)	Mg^{2+} (mg/L)	NH_4-N (mg/L)	Ca^{2+} (mg/L)	K^+ (mg/L)
Raw wastewater (after primary settling)	7.7±0.1	174±1	5.4±0.5	8.6±0.3	33±2.6	36.0±1.6	22.0 ±1.9
Wastewater suitable for bio-struvite formation (previously reported)	7.5–7.8	NP	30.5–41	38.9–74	336–629	NP	NP
Wastewater after addition of nutrients	7.7±0.1	715±16[a]	34.3±0.6[b]	55.2±0.4[c]	311.5 ±1.4[d]	36.6±0.4	93.1±1.1

[a] bovine serum albumin (BSA) (0.5 g/L); [b] di-potassium hydrogen phosphate (K_2HPO_4); [c] magnesium sulphate heptahydrate ($MgSO_4{\cdot}7H_2O$); [d] ammonium chloride (NH_4Cl) were added to the wastewater. NP-not provided.

Table 2 Bio-struvite production and changes of PO_4-P, NH_4-N, Mg^{2+}, Ca^{2+} concentrations and pH in the presence of microbial strains and in the non-inoculated control at the end of 192h incubation

	H. salinarum	*B. antiquum*	*M. xanthus*	*B. pumilus*	*I. loihiensis*	control
Bio-struvite production (mg bio-struvite [a]/L wastewater treated)	154±5	130±4	93±5	125±6	119±3	0
SCOD reduction	148±4 mg/L	316±4 mg/L	241±4 mg/L	237±7 mg/L	172±4 mg/L	0
pH increase	0.6±0.0	0.7±0.0	0.6±0.0	0.6±0.0	0.6±0.0	<0.1
NH_4-N production	41±1 mg/L	57±1 mg/L	49±0 mg/L	47±1mg/L	30±3 mg/L	<1 mg/L
PO_4-P removal	26±0 mg/L 76%	27±0 mg/L 79%	24±1 mg/L 71%	26±0 mg/L 75%	23±1 mg/L 66%	<1 mg/L 0%
Mg^{2+} removal	21±1 mg/L 38%	19±0 mg/L 42%	17±1 mg/L 31%	21±0 mg/L 38%	17±0 mg/L 30%	<1 mg/L 0%
PO_4-P recovered as bio-struvite[a]	19 mg/L 56%	16 mg/L 47%	12 mg/L 36%	16mg/L 46%	15 mg/L 43%	0 0%
Mg^{2+} recovered as bio-struvite[a]	15 mg/L 27%	13 mg/L 29%	9 mg/L 16%	12 mg/L 22%	12 mg/L 21%	0 0%

[a] Bio-struvite crystal ≥10 μm

Table 3 Key features of bio-struvite mineralization mechanisms by *H. salinarum, B. antiquum, B. pumilus, M. xanthus and I. loihiensis* in wastewater.

Evidence supporting biologically induced mineralization	
H. salinarum, *B. pumilus,* *M. xanthus*	-pH increase -NH_4-N production -Crystal morphology heterogeneity -Crystal size heterogeneity: *H. salinarum:* D_{v90}–D_{v50}=273 μm *B. pumilus:* D_{v90}–D_{v50}=257 μm *M. xanthus:* D_{v90}–D_{v50}=264 μm -Crusted cell structure for *B. pumilus*
Evidence supporting biologically controlled mineralization	
B. antiquum, *I. loihiensis*	-pH increase -NH_4-N production -Crystal morphology homogeneity *B. antiquum*: D_{v90}–D_{v50}=123 μm *I. loihiensis:* D_{v90}–D_{v50}=127 μm -Intracellular vesicle-like structures with electron-dense material

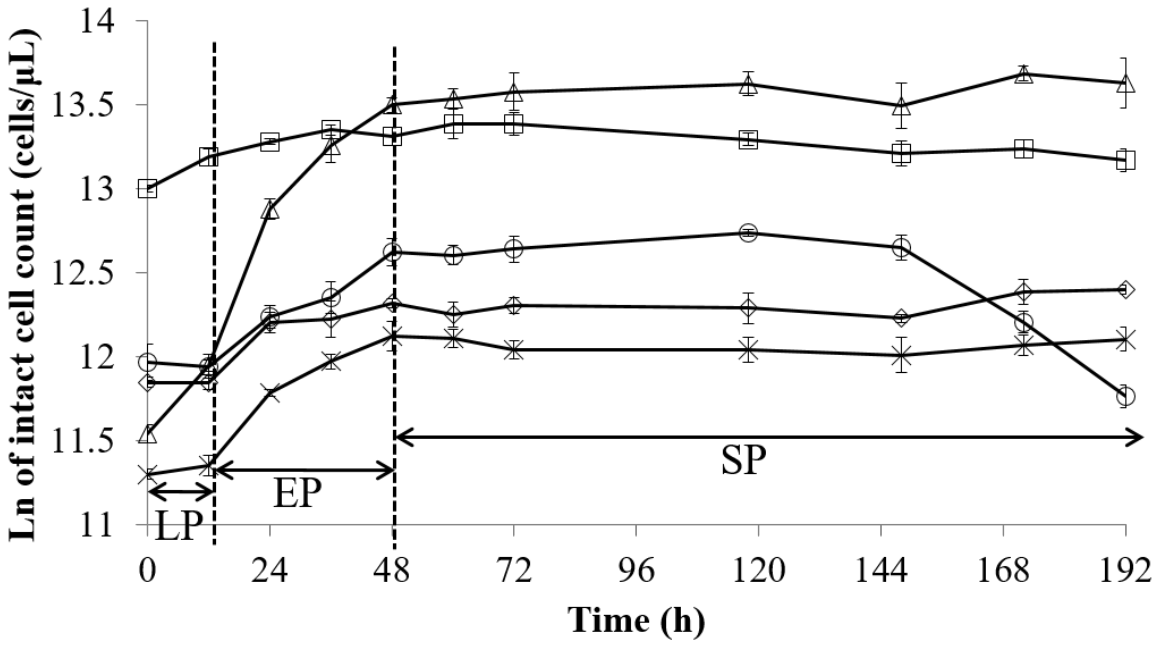

Fig. 1 Natural logarithm of intact cell counts of *H. salinarum* (×), *B. antiquum* (Δ), *B. pumilus* (◊), *M. xanthus* (○), *I. loihiensis* (□) in wastewater over 192 h incubation time. Error bars represent standard deviation obtained from duplicate tests (LP- lag phase, EP- exponential phase, SP- stationary phase of growth).

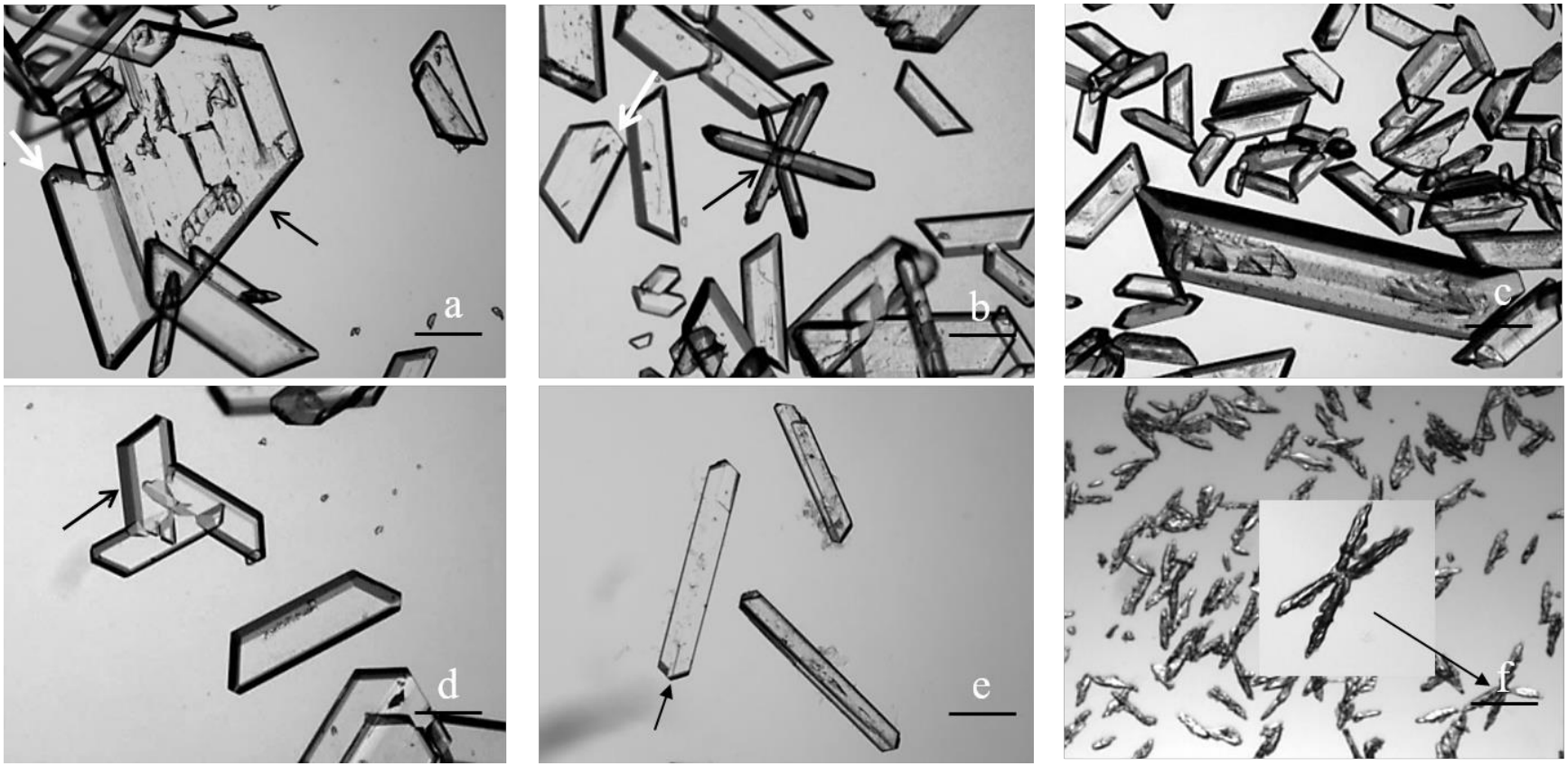

Fig. 2 Bio-struvite crystals produced during stationary phase of growth (118 h) by (a) *H. salinarum*, parallel grouping (black arrow), truncated apex (white arrow); (b) *B. pumilus*, penetrate twining (black arrow), truncated apex (white arrow); (c) *M. xanthus*; (d) *B. antiquum*, cyclic twining (black arrow); (e) *I. loihiensis*, contact twinning (black arrow). (f) Abiotic struvite, X-shaped (black arrow). Bar scale – 88.32 µm.

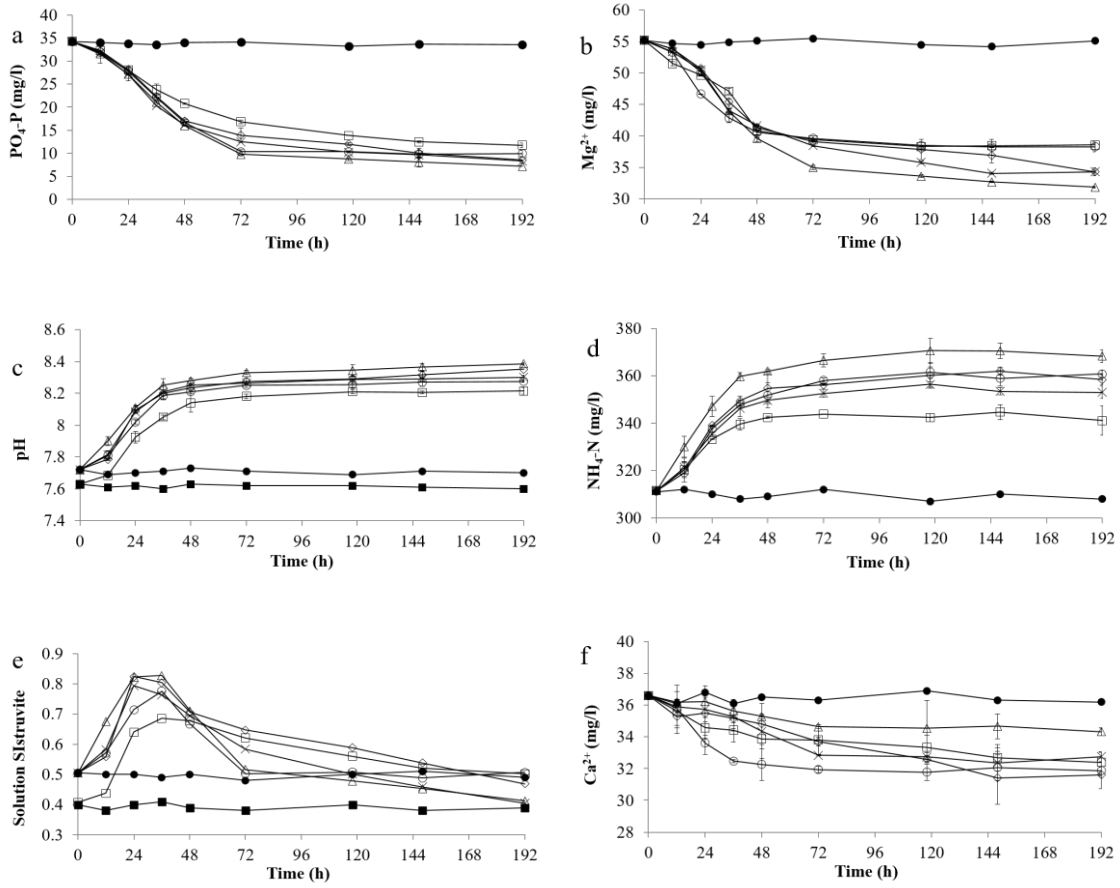

Fig. 3 Variations in PO_4-P (a), Mg^{2+} (b), pH (c), NH_4-N (d), solution $SI_{struvite}$ (e) and Ca^{2+} (f) in wastewater during cultivation of *H. salinarum* (×), *B. antiquum* (Δ), *B. pumilus* (◊), *M. xanthus* (○), *I. loihiensis* (□) and non-inoculated controls (● – wastewater, ■ – wastewater with additional 0.8% NaCl) with time (error bars represent standard deviation obtained from duplicates).

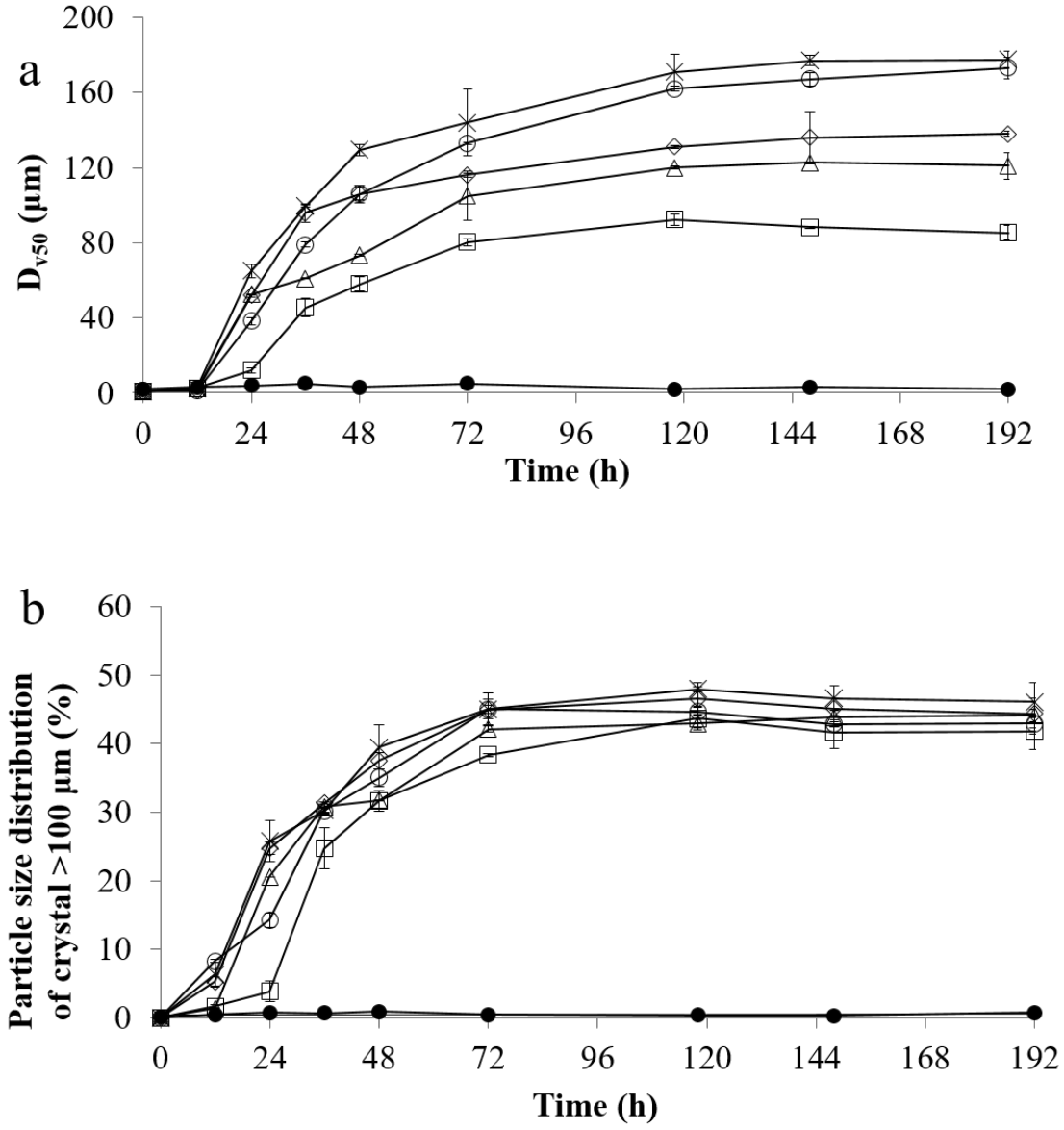

Fig. 4 Variation of D_{v50} (particle diameter at 50% in cumulative distribution on the basis of volume) (a) and percentage of crystal size >100 µm (b) in the presence of *H. salinarum* (×), *B. antiquum* (Δ), *B. pumilus* (◊), *M. xanthus* (○) and *I. loihiensis* (□) in wastewater and non-inoculated controls (●) with time (error bars represent standard deviation obtained from duplicates). D_{v50} is the value of particle diameter at 50% in the cumulative particle size distribution on a volume basis.

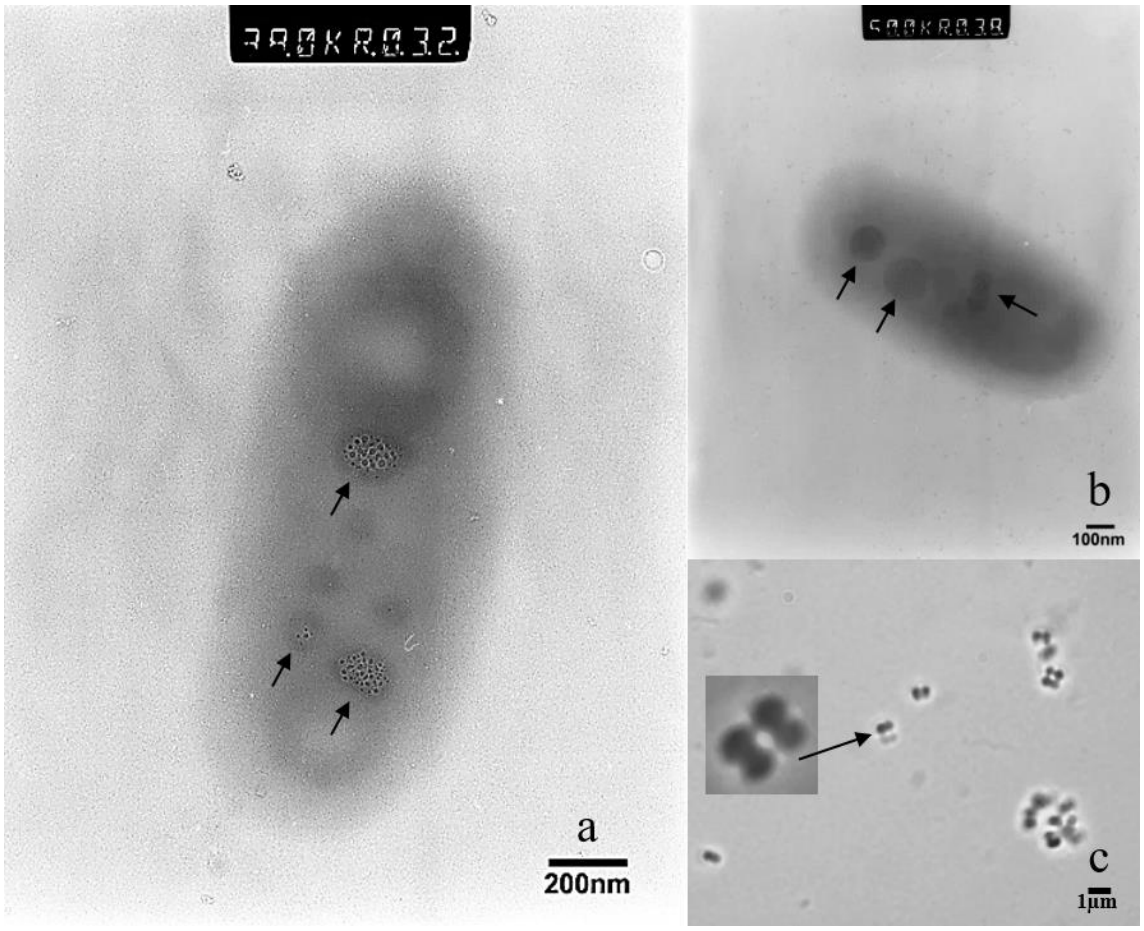

Fig. 5 TEM photo shows membrane-enclosed electron-dense granules/materials (arrow) inside *B. antiquum* cell and (b) *I. loihiensis* cells in wastewater (60 h). (c) Optical microscope photograph showing crusted cell structures (arrow) in *B. pumilus* culture (60h).

2021-07-24

The mechanisms of struvite biomineralization in municipal wastewater

Leng, Yirong

Elsevier

Leng Y, Soares A. (2021) The mechanisms of struvite biomineralization in municipal wastewater. Science of the Total Environment, Volume 799, December 2021, Article number 149261 10.1016/j.scitotenv.2021.149261